

Yu.V. Yavorskyi¹, Ya.V. Zaulychnyy¹, M.V. Karpets², A.B. Hrubciak³, V.V. Moklyak³,
O.I. Dudka¹, Ya.A. Kononenko¹

Changes in the Structural and Morphological Parameters of Fe₂O₃/SiO₂, as a Basis for the Electrode Material of Lithium Power Sources, Due to Shock-Vibrating Treatment

¹National Technical University of Ukraine "Igor Sikorsky Kiev Polytechnic Institute", Kyiv, Ukraine, yar-vra@ukr.net.

²National Academy of Sciences of Ukraine. Institute of Problems of Materials Science named after. Frantsevich, Kyiv, Ukraine, mkarpets@ukr.net.

³National Academy of Sciences of Ukraine. Institute of Metal Physics. GV Kurdyumova Blvd. Kyiv, Ukraine, hrubiakOandrii@gmail.com.

Using the method of X-ray diffraction, the effect of shock-vibration treatment on the structural parameters and phase composition of mixtures of silicon dioxide and alpha iron oxide was studied. From these results, has been found that the shock-vibration treatment of oxides mixture leads to an increase in the coherent scattering region of crystalline α -Fe₂O₃. We obtained SEM images of composites before and after treatment. From the SEM images it is seen that the processing is accompanied by fragmentation of the aggregates, uniform placement of the nanoparticles between each other and the formation of new denser agglomerates. Electron-microscopic study of mixtures using TEM was performed, which showed that the treatment leads to a lay-up of particles each other with the formation of interatomic interaction between them, which is consistent with the results of ultra-soft X-ray emission spectroscopy. The electrochemical properties of LPS, with electrodes based on mixtures before and after treatment, in galvanostatic mode were investigated. It is found that the charge capacity of the LPS with the electrode based on the mixture with the maximum concentration of α -Fe₂O₃ after treatment is reduced by half. In addition, such LPS doesn't have the following cycling, which is most likely to be associated with an increase in the recombination probability of lithium ions on the surface of the electrode material due to the increase in the population of Op-electrons near the Fermi level and compaction of the nanocomposite.

Keywords: SiO₂, α -Fe₂O₃, scanning electron microscopy, transmission electron microscopy, X-ray diffraction analysis, structure, lattice parameters, coherent scattering region, morphology, discharge capacity.

Стаття постуила до редакції 22.11.2019; прийнята до друку 15.12.2019.

Introduction

The intensive development of scientific and technological progress requires the use of new materials with unique predefined properties, such as high sorption capacity, superconducting properties, high ability to accumulate electric charge, etc. Given the intensive development of electro cars engineering and the increasing number of portable electronics, there is a need to use portable energy sources with high rates of charge capacity and cycling. Lithium power sources (LPS) are currently one of the most promising [1-9]. Therefore, it is

safe to say that the search for new electrode materials [2, 3, 5, 8, 9] that would provide the above mentioned features is undoubtedly an urgent task. It is known that the properties of materials, including the electrochemical properties of LPS, depend on the electronic structure of materials and the type of interatomic interaction of atoms [10-14] in crystalline, amorphous or molecular structures. A particular structure had been formed in the process of using certain methods of synthesis or processing. Therefore, to simplify the above problem, it is very important to understand how the valence electron distribution, morphology and structure of electrode materials in the process of their preparation changes, and

what the relationship between these parameters and the electrochemical properties of LPS [13, 14]. Based on this, the paper presents the change of structure-morphological features as a result of treatment at microbraker (MBT) is presented and the relationship between the change of these features, the change of the distribution of valence electrons and the charge capacities of the LPS with electrodes based on mixtures before and after treatment is established.

I. Materials and methods of research

The investigated samples of silicon oxide and titanium were synthesized at the Institute of Surface Chemistry, O.O. Chukha National Academy of Sciences of Ukraine.

The raw materials for the pyrogenic silicon dioxide were SiCl₄, which was fed into O₂/H₂ flames for hydrolysis/oxidation and the formation of nanoparticles of individual SiO₂ oxides with a specific surface area of 230 m²/g.

Synthesis of hematite (α -Fe₂O₃) was carried out by thermal decomposition of hydrated oxalate of iron (III) - Fe₂(C₂O₄)₃·5H₂O - in the temperature range of 350 - 370°C in the presence of oxygen. The thermal decomposition of hydrated iron oxalate was passed through the stepwise removal of crystallization water (endo-effect) followed by an exothermic process of decomposition of the salt to α -Fe₂O₃. The yield of this α -Fe₂O₃ synthesis method was approximately 35 %.

The mechanical treatment at microbraker (MBT) of mixtures of x-(SiO₂) + y-(α -Fe₂O₃) (where x-, y- is the corresponding mass content of the component) was performed in a mechanical vibration mill in Ardenne (Germany). MBT occurred in a metal reactor with a diameter of 25 mm using a single metal ball with a diameter of 10 mm, at a frequency of oscillation of the reactor 50 Hz. All MBT samples were prepared in a vibrating mill during 5 minutes.

Preparation of the initial mixtures was performed by conventional stirring for 5 minutes, followed by stirring in a 50 Hz mechanical vibrator Ardenne (Germany) in a 25 mm diameter metal reactor using one 10 mm diameter metal ball during 3 seconds.

Considering that, in the article [15], the mechanisms of electrochemical changes are not fully understood from the results of the study of the changes of structural features investigated by X-ray diffraction (XRD) analysis and the electronic structure investigation by ultra-soft X-ray emission spectroscopy (USXES). Therefore, it is necessary to use SEM and TEM for a more detailed investigation of the morphology and a detailed analysis of the results of X-ray diffraction analysis, namely changes in CSR, phase composition and lattice parameters.

Surface and morphology studies, as well as the determination of the chemical composition of the mixtures, were performed using a REM-106I scanning electron microscope (SELMI, Ukraine). Surface images of study objects were obtained with high spatial resolution and depth of field in reflected and secondary electrons. High-vacuum resolution is 4 nm. Pictures at

magnifications of x100, x250, x500, x1000 and x2500 were taken for a detailed study of the morphology and microstructure.

The studies of the morphology and structure of the mixtures were carried out on a transmission electron microscope Selmi 125 K in the center of electron microscopy at faculty of Physics and Engineering Igor Sikorski Kyiv Polytechnic institute. All the test specimens were deposited on a copper mesh with a carbon film.

X-ray diffraction studies were performed using CuK α monochromatic radiation on a DRON-UM1 diffractometer to determine the effect of UVO on crystal-structural parameters. As a monochromator used a single crystal of graphite mounted on a diffracted beam. The diffraction patterns were obtained by step scanning in the range of angles 2 θ 10-90° with a scan step of 0.05° and an exposure time of 3 - 7s. The experimental data were processed in Powder Cell 2.4. The studies were conducted at the Frantsevich Institute of Materials Science.

The study of electrochemical properties was carried out in the laboratories of the V. Stefanik Precarpathian National University. One of the most important electrochemical properties is cyclicality and charge/discharge capacity. After all, the longevity of use and cost-effectiveness of manufacturing LDS will depend on these parameters.

The study of charge capacities was carried out on a universal stand to investigate the intercalation properties of TIONiT P2.00 LV in galvanostatic mode [16]. The voltage range was chosen taking into account the chemical potentials of the electrode material and the anode material (metallic Li). In determining the optimal charge/discharge capacity, a current of 0.1 was selected from the theoretically calculated specific capacitance of the LDS (0.1C). The results were processed using Microsoft Excel and OriginPRO.

II. Results and discussion

X-ray phase analysis of the samples [15] showed that the phase composition of the samples before and after treatment remains within the error of the experiment, but the size of the CSR decreases. On the other hand, CSR is increasing. In addition, an increase in the SiO₂ content causes an increase in the degree of grinding of α -Fe₂O₃ when treated from a value of 8 nm in a mixture with an α -Fe₂O₃ content of 80 wt. % to 22 nm in a mixture with α -Fe₂O₃ 20 wt. %. In addition, it is established (Fig. 1) that the parameters of the lattice "a" and "c" as a result of MBT are within the error of the experiment (Table 1).

The authors of [14] showed that from the SEM images of the original α -Fe₂O₃ and after MBT, the particles of iron oxide are ground into smaller ones. At the same time, the MBT of amorphous SiO₂ is accompanied by a small grouping of particles.

A point-by-point chemical analysis was performed for a more detailed understanding. According to the research, crystallites of more regular shape and lighter color are found to be iron oxide, whereas cloud-like groupings are silicon oxide.

Table 1

Lattice parametrs (a,c) and changing the lattice parameters (Δ) as a result of MBT mixtures $\text{SiO}_2 + (\alpha\text{-Fe}_2\text{O}_3)$

Sample	$0.2\text{SiO}_2 + 0.8\text{Fe}_2\text{O}_3$		$0.5\text{SiO}_2 + 0.5\text{Fe}_2\text{O}_3$		$0.2\text{SiO}_2 + 0.8\text{Fe}_2\text{O}_3$		Fe_2O_3	
	a, nm	c, nm	a, nm	c, nm	a, nm	c, nm	a, nm	c, nm
Initial	0.5034	1.3746	0.5035	1.3747	0.5034	1.3748	0.5033	1.3745
After MBT	0.5035	1.3751	0.5036	1.3751	0.5037	1.3755	0.5035	1.3750
Δ	0.0001	0.0005	0.0001	0.0004	0.0003	0.0007	0.0002	0.0005
Error	0.0005 nm							

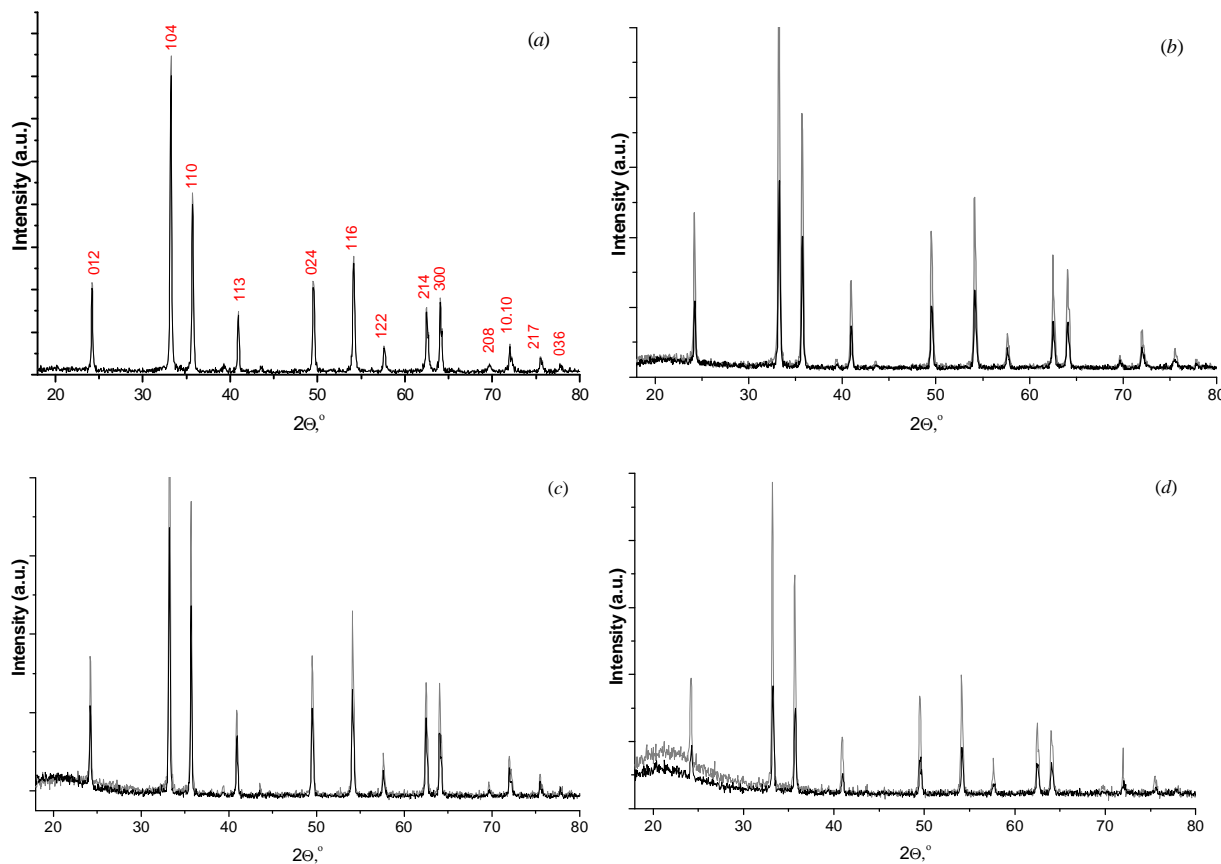


Fig. 1. X-ray diffraction pattern of initial mixture (gray line) and after MBT (black line): *a* - Fe_2O_3 . *b* - $0.2\text{SiO}_2 + 0.8\text{Fe}_2\text{O}_3$. *c* - $0.5\text{SiO}_2 + 0.5\text{Fe}_2\text{O}_3$. *d* - $0.8\text{SiO}_2 + 0.2\text{Fe}_2\text{O}_3$.

In (Fig. 2) the SEM image of mixtures of oxides with different mass ratios of components before and after MBT are presented. The image of the original mixture of 20 % $\text{SiO}_2 + 80\%$ $\alpha\text{-Fe}_2\text{O}_3$ shows that the silica nanoparticles are evenly distributed between the larger crystalline $\alpha\text{-Fe}_2\text{O}_3$ particles. At the same time, at the mixture after MBT we can see formation of agglomerates up to 60 μm in size from the particles of both oxides, which can indicate the formation of interaction between the particles of silicon and iron oxides [15]. In addition, as a result of MBT of the same mixture, the crushing of all crystallites of iron oxide to a size of less than 3 μm , which is significantly larger than the crushing that occurs with MBT of the original $\alpha\text{-Fe}_2\text{O}_3$. Similar grinding of $\alpha\text{-Fe}_2\text{O}_3$ particles is also present in mixtures with a concentration of 50 and 80 wt. % Fe_2O_3 , but it size are slightly larger, namely 1-8 and 1-7 microns, respectively. In addition, the size of the agglomerates after MBT of these mixtures is smaller and has a value of up to 35 and 30 μm , respectively.

The (Fig. 3) TEM image of a mixture with a SiO_2

content of 80 wt. % before and after MBT. When considering these images, the initial mixture of 80 % $\text{SiO}_2 + 20\%$ $\alpha\text{-Fe}_2\text{O}_3$ shows that amorphous SiO_2 particles of 7-9 nm in size and crystalline $\alpha\text{-Fe}_2\text{O}_3$ particles of 200 - 500 nm apart are evenly distributed between each other. At the same time after MBT there are a grinding of iron oxide particles to 100 - 250 nm. In addition, it should be noted that the shape of $\alpha\text{-Fe}_2\text{O}_3$ particles after MBT is more spherical. In addition, a layer of SiO_2 nanoparticles on the surface of $\alpha\text{-Fe}_2\text{O}_3$ nanoparticles is observed in the mixture after MBT (Fig. 3 (d)).

The (Fig. 4) presents the discharge curves of LPS with electrodes based on a mixture of 80 % $\text{SiO}_2 + 20\%$ Fe_2O_3 before and after MBT. From the discharge curve of the electrochemical cell with the electrode material based on the initial mixture shows that there is a sharp discharge from the potential difference of 4 V to 1.8 - 1.9 V and a slow reduction of the potential difference to 1 V and the specific capacity of 433.8 A·h/kg.

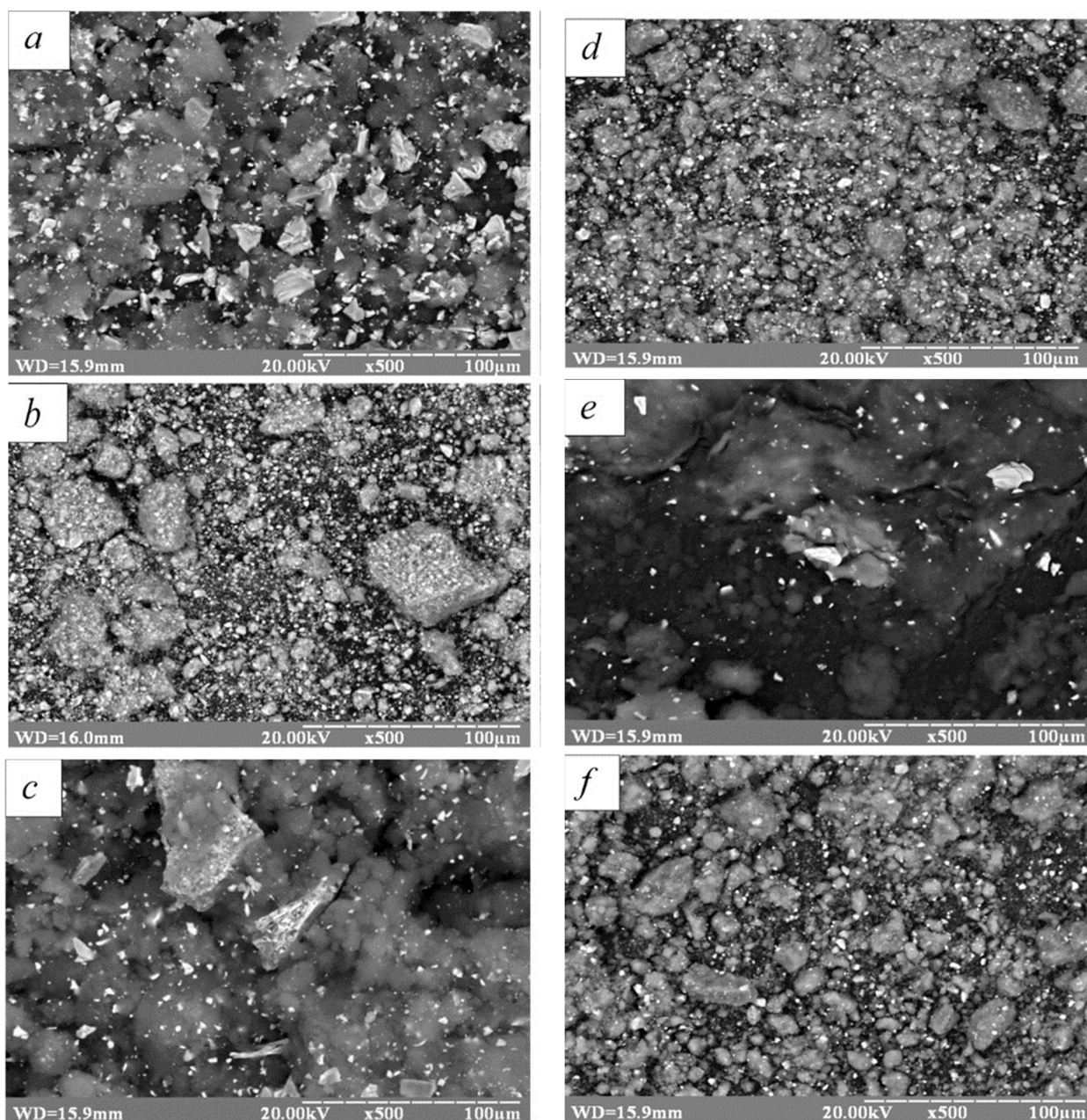


Fig. 2. SEM images of nanocomposites, with different mass ratios of components before (*a, c, e*) and after (*b, d, f*) treatment x500. (*a, b*) – 80 % Fe₂O₃ + 20 % SiO₂; (*c, d*) – 50 % Fe₂O₃ + 50 % SiO₂; (*e, f*) – 20 % Fe₂O₃ + 80 % SiO₂.

In the cell with the electrode based on the mixture after MBT, a sharp drop in the potential difference occurs to a value of 3.1 V, and the gentle discharge to 1 V ends at a value of specific capacity 874.9 A·h/kg. From these data, we can conclude that the specific capacity of the cell with the electrode material based on the initial mixture is less than 2.02 times the capacity of the cell with the electrode of the mixture after MBT. In this case, the power of the cell after MBT of base electrode material increases 2.35 times. This is most likely due to the decrease in particle size and the increase in electron density in the oxygen *p*-states. However, the presence of leaps in potential difference on the discharge curve of the LPS with the electrode after MBT indicates the processes of recombination of lithium ions on the electrode material.

This are well corroborated by the results of

galvanostatic cycling of the LPS with the electrodes based on a mixture of 20 % SiO₂ + 80 % Fe₂O₃ before and after MBT.

The (Fig. 5) presents the discharge curves of the LPS with electrodes based on a mixture of 20 % SiO₂ + 80 % Fe₂O₃ before and after MBT. When considering the discharge curves of LPS with electrodes based on the initial mixture with an iron concentration of 80 wt. % shows that the capacity of the cell are 119.5 A·h/kg, the next cycling of LPS there are a decrease in the charge capacity to 47 A·h/kg and stabilization of this value in subsequent cycles. At the same time at the LPS with electrode based on mixture

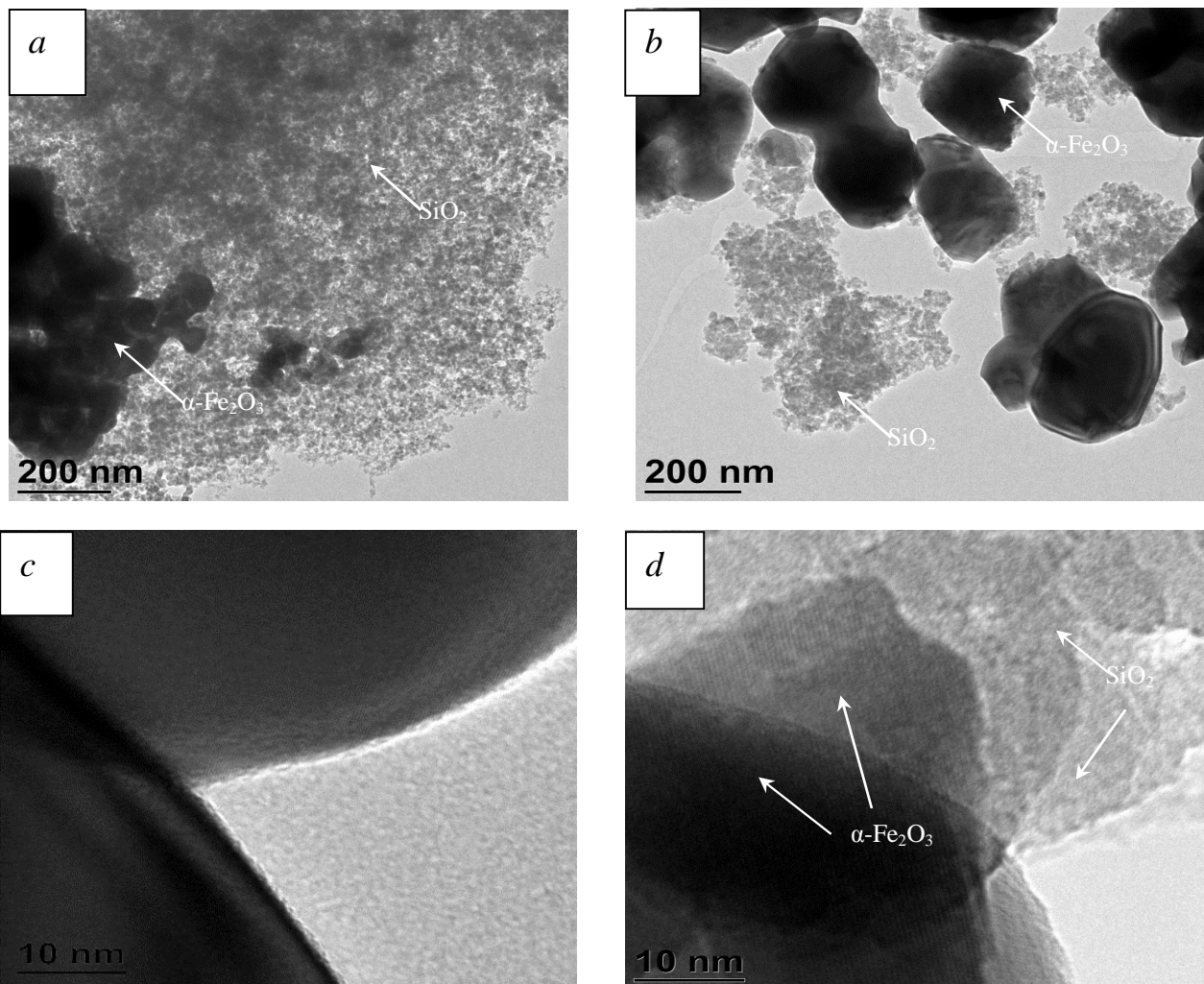


Fig. 3. TEM images 80%SiO₂+20% α -Fe₂O₃ mixture before (a, c) and after MBT (b, d).

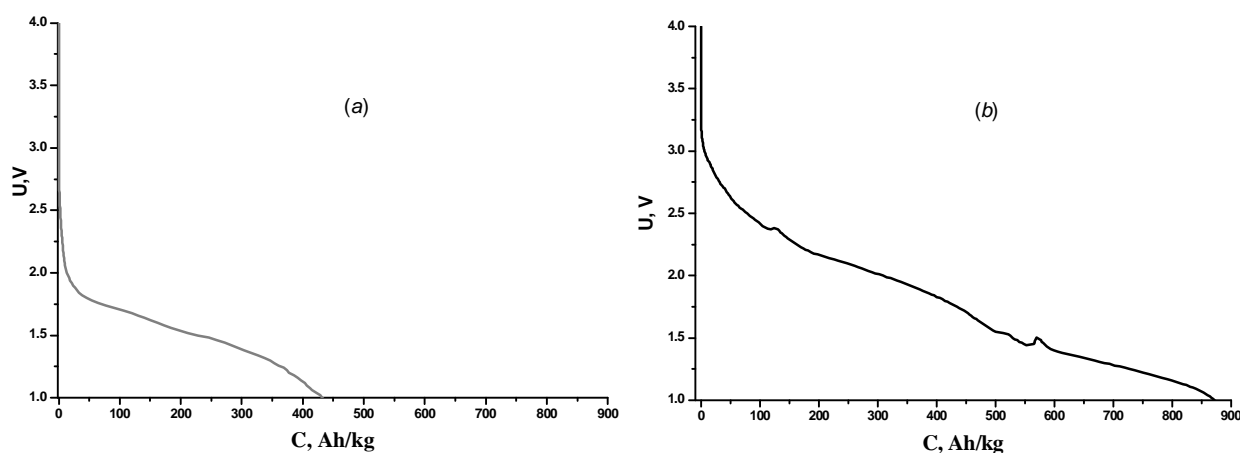


Fig. 4. The discharge curves of the mixture 80 % SiO₂ + 20 % Fe₂O₃ before (a) and after MBT (b).

ter MBT discharge up to a potential difference of 1.6 V and a capacity of 27 A·h/kG. Subsequently, the discharge was accompanied by sudden changes in voltage and its decrease to 1.18 V and the formation of another shelf at this voltage. In this case, the discharge occurs at an unstable voltage up to a small value of the discharge capacity 52 A·h/kg. Subsequently, LPS doesn't have

cycling. A similar effect are observed for LPS with an electrode based on a mixture with concentration of α -Fe₂O₃ 20 wt. % after MBT, on the discharge curve of which in the region (508 ÷ 590) A·h/kg there are jumps of potential difference, which is a consequence of the formation of oxide groups on the surface of the electrode material.

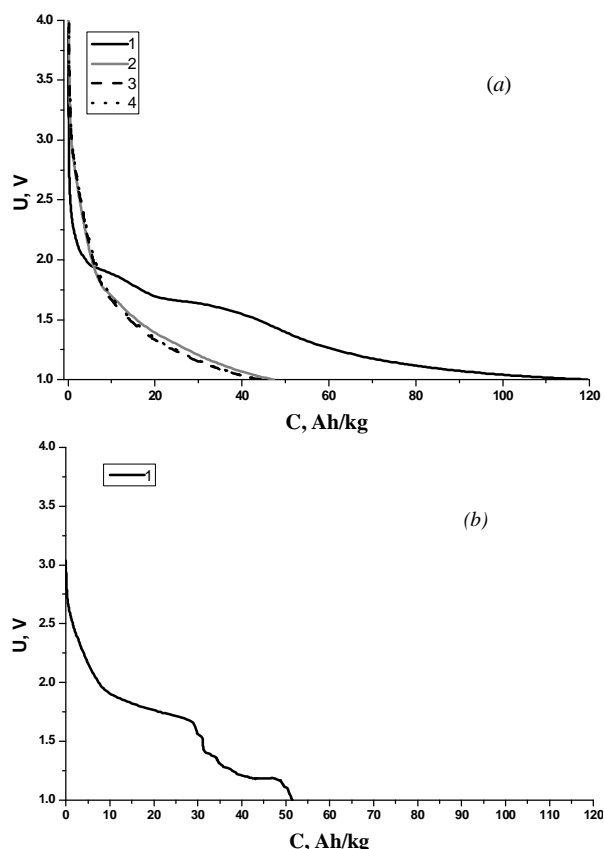


Fig. 5. The discharge curves of the 20 % SiO₂ + 80 % Fe₂O₃ mixture before (a) and after MBT (b).

This indicates that an increase in electron density near the ceiling of the valence band [15] leads to an increase in the probability of the formation of an interatomic interaction between the surface oxygen anions and lithium cations (recombination of lithium ions on the surface and in the pores of the electrode material). This is a favorable condition for the further formation of a passive film around the particles of the electrode material, which is only accompanied by a decrease in the charge capacity of the LPS with the electrode based on the mixture after MBT.

Conclusion

Due to the MBT of mixtures of SiO₂ + α -Fe₂O₃, with different mass ratios of components, there are a grinding of α -Fe₂O₃ nanoparticles, which are accompanied by a decrease in the CSR. In the future, the formation of new agglomerates, which includes both particles SiO₂ and α -Fe₂O₃.

The results of the TEM image analysis show that due to the high local pressures that accompany the MBT process, the oxide nanoparticles are layered each other.

From the results of galvanostatic cycling and ultra-soft X-ray emission spectroscopy, show that, an increase in the electron density in the oxygen *p*-states of the electrode material causes an increase in the LPS discharge capacity. However, an increase in the electron density in the high-energy zone of the *Op*-states near the ceiling of the valence band causes an increase in the likelihood of recombination of lithium ions on the surface of the cathode material into oxide groups, which interfere with the intercalation of lithium ions into structural channels and voids.

Yavorskiy Y.V. – PhD., assoc. Prof. Department Of Metal Science And Heat Treatment Faculty Of Engineering And Physics Igor Sikorsky Polytechnic Institute

Zaulychnyy Y.V. – Doctor Of Science, Full Prof., Head of Department Of Metal Science And Heat Treatment Faculty Of Engineering And Physics Igor Sikorsky Polytechnic Institute;

Karpets M.V. – Doctor Of Science, Full Prof. Department Of Metal Science And Heat Treatment Faculty Of Engineering And Physics Igor Sikorsky Polytechnic Institute;

Hrubiak A.B. – PhD., Researcher of Institute of Metal Physics. GV Kurdyumova

Moklyak V.V. – Doctor Of Science, Senior Researcher of Institute of Metal Physics. GV Kurdyumova

Dudka O. I. – assoc. Prof. Department Of Metal Science And Heat Treatment Faculty Of Engineering And Physics Igor Sikorsky Polytechnic Institute;

Kononenko Ya.A. – Student Department Of Metal Science And Heat Treatment Faculty Of Engineering And Physics Igor Sikorsky Polytechnic Institute.

- [1] Yong-mao Lin, Paul R. Abel, Adam Heller, and C. Buddie Mullins, *J. Phys. Chem. Lett.* 2, 2885 (2011).
- [2] Yuzheng Guo, Stewart J Clark, John Robertson, *J. Phys.: Condens. Matter.* 24, 8 (2012).
- [3] Li Xu, Yuhui Tian, Tiefeng Liu, Henan Li, Jingxia Qiu, Sheng Li, Huaming Li, Shouqi Yuan, Shanqing Zhang, *Green Energy and Environment*, S2468-0257(17)30184-X (2018).
- [4] Jose Balbuena, Manuel Cruz-Yusta, Adri an Pastor, Luis Sanchez, *Journal of Alloys and Compounds* 735, 1553 (2018).
- [5] Gaurav Jain, Mahalingam Balasubramanian and Jun John Xu, *Chem. Mater.* 18, 423 (2006).
- [6] X.L. Gou, G.X. Wang, X.Y. Kong, D. Wexler, J. Horvat, J. Yang, J. Park, *Chem. - Eur. J.* 14, 5996 (2008).
- [7] G.X. Wang, X.L. Gou, J. Horvat, J.J. Park, *Phys. Chem. C* 112, 15220 (2008).
- [8] Andrii B. Hrubiak, Volodymyr O. Kotsyubynsky, Volodymyr V. Moklyak, Bogdan K. Ostafiychuk, Pavlo I. Kolkovsky, Sofia V. Fedorchenko & Bogdan I. Rachiy, *Molecular Crystals and Liquid Crystals*, 670:1, 97 (2018) (DOI: 10.1080/15421406.2018.1542070).

- [9] Volodymyr Kotsyubynsky, Bogdan Ostafiychuk, Volodymyr Moklyak and Andrii Hrubiak, *Solid State Phenomena* 230, 120 (2015).
- [10] Yan Zhong, Yifan Ma, Qiubo Guo, Jiaqi Liu, Yadong Wang, Mei Yang & Hui Xia, *Scientific RepoRts*, 7:40927, (2017) (DOI: 10.1038/srep40927).
- [11] P.G. Bruce, B. Scrosati, & J.M. Tarascon, *Angew. Chem. Int. Ed.* 47, 2930 (2008).
- [12] H. Wu, & Y. Cui, *Nano Today* 7, 414 (2012).
- [13] Ya.V. Zaulychnyy, V.M. Gun'ko, Y.V. Yavorskyi, I.M. Gasyuk, N. Wanderka, O.I. Dudka, *Applied Surface Science* 494, 1013 (2019).
- [14] Yu.V. Yavorsky, Ya.V. Zaulichny, V.M. Gunko, M.V. Karpets, *Journal Of Nano- And Electronic Physics* 10, 6, 06005 (2018).
- [15] Ya.V. Zaulychnyy, V.M. Gun'ko, Yu.V. Yavorskyi, V.I. Zarko, S.S. Piotrowska, V.M. Mishchenko, *Metallofiz. Noveishie Tekhnol.* 37(8), 1063 (2015).
- [16] Yu.V. Yavorsky, Ya.V. Zaulichny, V.M. Gunko, M.V. Karpets, V.V. Mokliak, *Journal of Nano- And Electronic Physics* 11, 6 (2018).

Ю.В. Яворський¹, Я.В. Зауличний¹, М.В. Карпець², А.Б. Груб'як³, В.В. Мокляк³,
О.І. Дудка¹, Я.А. Кононенко¹

Зміна структурно-морфологічних параметрів Fe₂O₃/SiO₂, як основи електродного матеріалу літєвих джерел струму, внаслідок ударно вібраційної обробки

¹Національний технічний університет України «Київський політехнічний інститут», Київ, Україна, yar-yra@ukr.net.

²Національна Академія Наук України. Інститут проблем матеріалознавства ім. Францевича, Київ, Україна, mkarpets@ukr.net.

³Національна Академія Наук України. Інститут металофізики ім. Г.В. Курдюмова, Київ, hrubiak0andrii@gmail.com.

Використовуючи метод рентгеноструктурного аналізу було вивчено вплив ударно-вібраційної обробки на структурні параметри та фазовий склад сумішей діоксидів кремнію та оксиду альфа заліза. З цих результатів встановлено, що ударно-вібраційна обробка суміші оксидів приводить до зростання області когерентного розсіювання кристалічного α -Fe₂O₃. Отримано СЕМ зображення композитів до та після обробки. З СЕМ зображень видно, що обробка супроводжується роздробленням агрегатів, рівномірним розміщенням наночастинок один між одними та утворенням нових більш щільних агломератів. Проведено електронно-мікроскопічне дослідження сумішей за допомогою ТЕМ, яке показало, що обробка приводить до нашарування частинок одна на одну з утворенням міжатомної взаємодії між ними, що узгоджується з результатами ультрам'якої рентгенівської емісійної спектроскопії. Проведено дослідження електрохімічних властивостей ЛДС, з електродами на основі сумішей до та після обробки, в гальваностатичному режимі. Встановлено, що зарядова ємність ЛДС з електродом на основі суміші з максимальним вмістом α -Fe₂O₃ після обробки зменшується в два рази. Крім того, в такому ЛДС відсутня наступна цикльованість, що найбільш імовірно пов'язано із збільшенням рекомбінаційної імовірності іонів літію на поверхні електродного матеріалу внаслідок збільшення заселеності Ор-електронів поблизу стелі валентної зони і ущільнення нанокompозиту.

Ключові слова: SiO₂, α -Fe₂O₃, скануюча електронна мікроскопія, трансмісійна електронна мікроскопія, рентгеноструктурний аналіз, структура, параметри ґратки, область когерентного розсіювання, морфологія, розрядна ємність.